
This copy is for your personal, non-commercial use only.

If you wish to distribute this article to others, you can order high-quality copies for your colleagues, clients, or customers by [clicking here](#).

Permission to republish or repurpose articles or portions of articles can be obtained by following the guidelines [here](#).

The following resources related to this article are available online at www.sciencemag.org (this information is current as of January 2, 2011):

Updated information and services, including high-resolution figures, can be found in the online version of this article at:

<http://www.sciencemag.org/content/314/5800/825.full.html>

Supporting Online Material can be found at:

<http://www.sciencemag.org/content/suppl/2006/10/30/314.5800.825.DC1.html>

A list of selected additional articles on the Science Web sites **related to this article** can be found at:

<http://www.sciencemag.org/content/314/5800/825.full.html#related>

This article has been **cited by** 58 article(s) on the ISI Web of Science

This article has been **cited by** 17 articles hosted by HighWire Press; see:

<http://www.sciencemag.org/content/314/5800/825.full.html#related-urls>

This article appears in the following **subject collections**:

Medicine, Diseases

<http://www.sciencemag.org/cgi/collection/medicine>

discriminate between the many possible high-resolution models by relying on the dichroism of the EXAFS spectra.

The structural changes of the Mn₄Ca complex on advancing through the S₁ state intermediates can be placed in the context of the polarized EXAFS data to assist in deriving a mechanism for photosynthetic water oxidation. The FTIR data, in conjunction with model II (Fig. 4), suggest that Mn_A, which may be ligated by Asp¹⁷⁰, does not change oxidation state and remains Mn(III) or Mn(IV) throughout the Kok cycle. The C-terminal Ala³⁴⁴ may be a ligand to Mn_D, which is proposed to undergo Mn(III)→Mn(IV) oxidation during the S₁→S₂ transition (26–28). Recent FTIR data suggest that His³³² monitors structural changes of the Mn₄Ca cluster, but no evidence for a Mn-centered oxidation was reported (29). Because Mn_C is closer to His³³², Mn_C may remain Mn(III) or Mn(IV) throughout the cycle. Consequently, Mn_B is a likely candidate for Mn oxidation during the S₀→S₁ transition.

The dichroism in the polarized EXAFS data from single crystals provides a powerful filter for choosing among many of the proposed structural models. Also, as shown in this study, the combination of XRD and polarized EXAFS on single crystals has several advantages for unraveling structures of x-ray damage-prone, redox-active metal sites in proteins. XRD structures at medium resolution are sufficient to determine the overall shape and placement of the metal site within the ligand sphere, and refinement by means of polarized EXAFS can provide accurate metal-to-metal and metal-to-ligand vectors. In addition, different intermediate states of the active site (including different metal oxidation states), which may be difficult to study with XRD at high resolution, can be examined. The structural model from polarized EXAFS from the S₁ state presented here, and from the other S states, will provide a reliable foundation for the investigation of the mechanism of photosynthetic water oxidation and for the design of biomimetic catalysts for water splitting.

References and Notes

1. T. Wydrzynski, S. Satoh, *Photosystem II: The Light-Driven Water: Plastoquinone Oxidoreductase*, *Advances in Photosynthesis and Respiration Series*, vol. 22 (Springer, Dordrecht, Netherlands, 2005).
2. B. Kok, B. Forbush, M. McGloin, *Photochem. Photobiol.* **11**, 457 (1970).
3. T. G. Carrell, A. M. Tyryshkin, G. C. Dismukes, *J. Biol. Inorg. Chem.* **7**, 2 (2002).
4. G. W. Brudvig, *Adv. Chem. Ser.* **246**, 249 (1995).
5. K. Hasegawa, T.-A. Ono, Y. Inoue, M. Kusunoki, *Chem. Phys. Lett.* **300**, 9 (1999).
6. J. M. Peloquin, R. D. Britt, *Biochim. Biophys. Acta* **1503**, 96 (2001).
7. J. Messinger, J. H. A. Nugent, M. C. W. Evans, *Biochemistry* **36**, 11055 (1997).
8. K. A. Åhrling, S. Peterson, S. Styring, *Biochemistry* **37**, 8115 (1998).
9. L. V. Kulik, B. Epel, W. Lubitz, J. Messinger, *J. Am. Chem. Soc.* **127**, 2392 (2005).
10. V. K. Yachandra, K. Sauer, M. P. Klein, *Chem. Rev.* **96**, 2927 (1996).
11. H.-A. Chu, W. Hillier, N. A. Law, G. T. Babcock, *Biochim. Biophys. Acta* **1503**, 69 (2001).
12. A. Zouni *et al.*, *Nature* **409**, 739 (2001).
13. N. Kamiya, J. R. Shen, *Proc. Natl. Acad. Sci. U.S.A.* **100**, 98 (2003).
14. K. N. Ferreira, T. M. Iverson, K. Maghlaoui, J. Barber, S. Iwata, *Science* **303**, 1831 (2004).
15. J. Biesiadka, B. Loll, J. Kern, K. D. Irrgang, A. Zouni, *Phys. Chem. Chem. Phys.* **6**, 4733 (2004).
16. B. Loll, J. Kern, W. Saenger, A. Zouni, J. Biesiadka, *Nature* **438**, 1040 (2005).
17. J. Yano *et al.*, *Proc. Natl. Acad. Sci. U.S.A.* **102**, 12047 (2005).
18. J. H. Robblee *et al.*, *J. Am. Chem. Soc.* **124**, 7459 (2002).
19. R. M. Cinco *et al.*, *Biochemistry* **41**, 12928 (2002).
20. R. M. Cinco *et al.*, *Biochemistry* **43**, 13271 (2004).
21. J. Yano *et al.*, *J. Am. Chem. Soc.* **127**, 14974 (2005).
22. R. A. Scott, J. E. Hahn, S. Doniach, H. C. Freeman, K. O. Hodgson, *J. Am. Chem. Soc.* **104**, 5364 (1982).
23. A. M. Flank, M. Weinger, L. E. Mortenson, S. P. Cramer, *J. Am. Chem. Soc.* **108**, 1049 (1986).
24. Materials and methods are available as supporting material on Science Online.
25. J. J. Rehr, R. C. Albers, *Rev. Mod. Phys.* **72**, 621 (2000).
26. H. A. Chu, W. Hillier, R. J. Debus, *Biochemistry* **43**, 3152 (2004).
27. R. J. Debus, M. A. Strickler, L. M. Walker, W. Hillier, *Biochemistry* **44**, 1367 (2005).
28. Y. Kimura, N. Mizusawa, T. Yamanari, A. Ishii, T. Ono, *J. Biol. Chem.* **280**, 2078 (2005).
29. Y. Kimura, N. Mizusawa, A. Ishii, T. Ono, *Biochemistry* **44**, 16072 (2005).

Supporting Online Material

www.sciencemag.org/cgi/content/full/314/5800/821/DC1

Material and Methods

SOM Text

Figs. S1 to S7

Tables S1 and S2

References

31 March 2006; accepted 14 June 2006

10.1126/science.1128186

Transgenic Mice with a Reduced Core Body Temperature Have an Increased Life Span

Bruno Conti,^{1,2*} Manuel Sanchez-Alavez,^{1,2} Raphaelle Winsky-Sommerer,^{3†} Maria Concetta Morale,^{1‡} Jacinta Lucero,^{1,2} Sara Brownell,^{1,2§} Veronique Fabre,^{3||} Salvador Huitron-Resendiz,² Steven Henriksen,^{2¶} Eric P. Zorrilla,^{1,2} Luis de Lecea,^{3#} Tamas Bartfai^{1,2}

Reduction of core body temperature has been proposed to contribute to the increased life span and the antiaging effects conferred by calorie restriction (CR). Validation of this hypothesis has been difficult in homeotherms, primarily due to a lack of experimental models. We report that transgenic mice engineered to overexpress the uncoupling protein 2 in hypocretin neurons (Hcrt-UCP2) have elevated hypothalamic temperature. The effects of local temperature elevation on the central thermostat resulted in a 0.3° to 0.5°C reduction of the core body temperature. Fed ad libitum, Hcrt-UCP2 transgenic mice had the same caloric intake as their wild-type littermates but had increased energy efficiency and a greater median life span (12% increase in males; 20% increase in females). Thus, modest, sustained reduction of core body temperature prolonged life span independent of altered diet or CR.

Temperature homeostasis in mammals is regulated centrally by neurons located in the preoptic area (POA) of the hypothalamus, a region that includes the medial and lateral part of the preoptic nucleus, the anterior hypothalamus, and the nearby regions of the septum. This region is believed to contain the central thermostat, which keeps core body temperature (CBT) within a very narrow range even when the animal is exposed

to a wide range of ambient temperatures. Lesion and thermal stimulation studies have demonstrated that the POA senses changes in local and peripheral temperatures and coordinates thermoregulatory responses [for review, see (1)].

With the aim of generating animals with a reduced CBT, we hypothesized that local heat production within or proximate to the POA, by mimicking an increase in CBT, might ac-

tivate compensatory thermoregulatory mechanisms and thereby reduce CBT. We generated mice that overexpressed the uncoupling protein 2 (UCP2) exclusively in hypocretin (Hcrt) neurons (Hcrt-UCP2 mice). UCP2 is an inner mitochondrial membrane protein that uncouples oxidative phosphorylation from respiration by leaking hydrogen ions from the intermembrane space to the matrix, thereby dissipating the proton gradient energy in the form of heat (2). Hypocretins (hypocretin 1 and 2), also known as orexins, are neuropeptides derived from a common precursor that participate in the regulation of the sleep/wake cycle, energy balance, food intake, and

endocrine and autonomic functions (3–5). Hypocretins are exclusively expressed in approximately 3000 neurons in the lateral hypothalamus (LH) at a distance of 0.8 mm from the POA (6) and provide an anatomically restricted site for heat generation in the hypothalamus.

A colony of Hcrt-UCP2 mice and wild-type littermates was established from one founder generated on and backcrossed for seven generations on a C57/BL6 background (fig. S1A).

To determine whether UCP2 overexpression in hypocretin neurons resulted in heat production that could affect the POA, we measured local temperature in the LH and in the POA. Local temperature was significantly higher in both the LH and the POA of Hcrt-UCP2 mice compared with wild-type mice (Fig. 1). Temperature elevation averaged 0.65°C in the LH and 0.32°C in the POA. The smaller increase in temperature elevation in the POA compared with the LH was likely due to heat dissipation from the LH. The difference between LH and POA temperature was constant during the 24 hours of recording.

The effect of elevated hypothalamic temperature on CBT was studied using radiotelemetry in male and female mice (Fig. 2). Hcrt-UCP2 mice maintained a normal circadian variation of CBT during the light and the dark cycles. In males, no difference in the CBT values between Hcrt-UCP2 and wild-type mice was observed during the light phase

or during the transition between phases. However, Hcrt-UCP2 mice consistently exhibited a significantly lower CBT during the dark phase throughout several days of recording (Fig. 2). In females, the reduction of CBT averaged 0.34°C and was more pronounced in the second part of the dark phase with a peak difference of 0.6°C (Fig. 2, A and B). A similar pattern was seen in male transgenics, with no difference observed during the light phase and the transition from light to dark, but an average CBT reduction of 0.3°C and a peak difference of 0.56°C observed during the dark phase (Fig. 2, D and E). In contrast to males, female Hcrt-UCP2 mice also showed a significant reduction of CBT in the first half of the transition from dark to light. Motor activity was similar between Hcrt-UCP2 and wild-type mice, being only marginally higher in Hcrt-UCP2 male mice at the end of the light-dark transition, a time when no difference in CBT was observed. In females, motor activity of Hcrt-UCP2 mice was marginally lower in the last part of the dark phase, when CBT also was lowest (Fig. 2, C and F). After injection with *Escherichia coli* lipopolysaccharides (LPS), Hcrt-UCP2 mice developed a fever response similar in amplitude and duration to that of the wild-type mice, which indicates that the thermogenic capacity of Hcrt-UCP2 mice was not impaired (fig. S3). The CBT profile was identical between transgenic and wild-type mice during the stress peak and the light phase, but Hcrt-UCP2 mice

¹Harold L. Dorris Neurological Research Center, Scripps Research Institute, La Jolla, CA 92037, USA. ²Molecular and Integrative Neurosciences Department, Scripps Research Institute, La Jolla, CA 92037, USA. ³Department of Molecular Biology, Scripps Research Institute, La Jolla, CA 92037, USA.

*To whom correspondence should be addressed. E mail: bcontini@scripps.edu

†Present address: Institute of Pharmacology and Toxicology, University of Zurich, Zurich, Switzerland.

‡Present address: Dipartimento di Neurofarmacologia, OASI (IRCCS), Troina, Italy.

§Division of Geriatric Medicine, Department of Medicine, UCSD, La Jolla, CA 92037, USA.

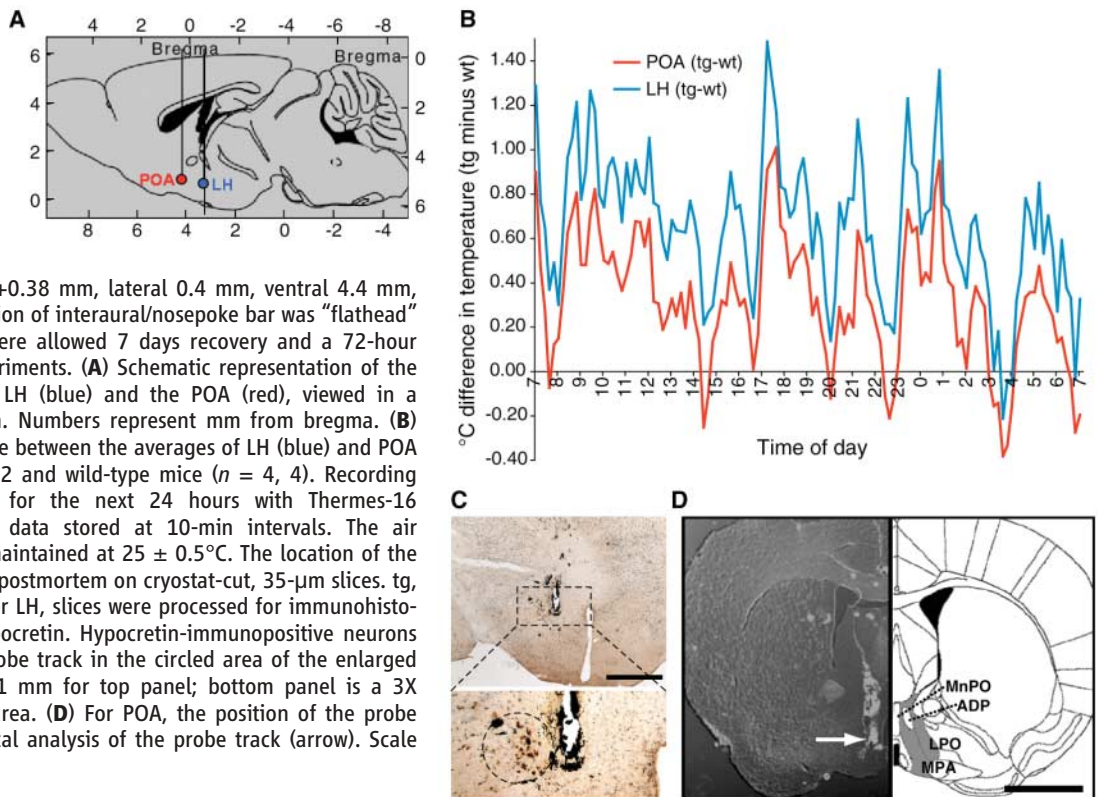
||Present address: Unité Mixte de Recherche 677, Institut National de la Santé et de la Recherche Médicale/Université Pierre et Marie Curie, Paris, France.

¶Present address: Western University of Health Sciences, Pomona, CA 91766, USA.

#Present address: Department of Psychiatry and Behavioral Sciences, Stanford University School of Medicine, Palo Alto, CA 94305, USA.

Fig. 1. UCP2 overexpression elevated local temperature. Three-month-old mice were stereotactically implanted with thermocouple probes in the lateral hypothalamic area (anteroposterior from bregma -0.7 mm, lateral 1.25 mm, ventral 4.5 mm, dura at point of entry) and the POA

(anteroposterior from bregma +0.38 mm, lateral 0.4 mm, ventral 4.4 mm, dura at point of entry; the position of interaural/nosepoke bar was “flathead” bregma = lambda). Animals were allowed 7 days recovery and a 72-hour habituation period before experiments. **(A)** Schematic representation of the location of the probes in the LH (blue) and the POA (red), viewed in a sagittal section of mouse brain. Numbers represent mm from bregma. **(B)** Profile of temperature difference between the averages of LH (blue) and POA (red) temperatures of Hcrt-UCP2 and wild-type mice ($n = 4, 4$). Recording was carried out continuously for the next 24 hours with Thermo-16 (Physitemp Instruments), with data stored at 10-min intervals. The air temperature in the room was maintained at $25 \pm 0.5^\circ\text{C}$. The location of the recording sites was determined postmortem on cryostat-cut, 35- μm slices. tg, transgenic; wt, wild-type. **(C)** For LH, slices were processed for immunohistochemistry with antibody to hypocretin. Hypocretin-immunopositive neurons are visible at the left of the probe track in the circled area of the enlarged detailed section. Scale bar is 1 mm for top panel; bottom panel is a 3X magnification of the selected area. **(D)** For POA, the position of the probe was demonstrated by histological analysis of the probe track (arrow). Scale bar, 2 mm.



maintained a temperature slightly higher than wild-type mice during the first half and the end of the dark phase. Overall, the data indicate that the reduction of basal CBT observed in Hcrt-UCP2 mice did not result from reduced locomotor activity or impaired thermogenic ability, but is consistent with an effect on the central thermostat.

We found that UCP2 overexpression reduced the number of hypocretin immunore-

active neurons by 22% and 30% in male and female Hcrt-UCP2 mice, respectively (fig. S4). It might be argued that intracellular temperature elevation, an excessive reduction in ATP synthesis, or altered intracellular Ca^{2+} concentrations resulting from UCP2 overexpression interferes with the normal metabolic activity of hypocretin neurons. Intracerebroventricular injection of pharmacologically high doses of hypocretin 1 reportedly ele-

vates spontaneous physical activity and CBT (7–10). However, the possibility that a decreased number of hypocretin neurons contributed to the reduced CBT was ruled out in orexin/ataxin-3 mice (11) that showed 90% reduction of hypocretin neurons but no significantly lowered CBT (fig. S5). No differences in sleep parameters that could account for the reduction of CBT were found (SOM text).

The effects of UCP2 overexpression in hypocretin neurons on water and food consumption were also measured. Hcrt-UCP2 mice did not differ from wild-type mice in their intake of chow (measured every 3 hours or biweekly) (Fig. 3A) or water ($M \pm SEM$: 3.7 ± 0.3 versus 3.6 ± 0.2 ml for wild-type and Hcrt-UCP2, measured biweekly). Whereas body weights of female Hcrt-UCP2 and wild-type mice did not significantly differ, male transgenic mice began to weigh significantly more than wild-type mice beginning at 20 weeks of age. By 35 weeks of age, the male transgenics weighed 10% more than the wild-type males (Fig. 3B). When subjected to 27 hours of food deprivation, Hcrt-UCP2 transgenic mice lost significantly less weight than would be predicted from their expected metabolic body mass demands as compared with wild-type littermates (genotype effect: $F(1,29) = 20.64$, $P < 0.0001$). The decrease in putative relative energy expenditure, which was similar in both male and female transgenics (Fig. 3C), is an index of increased metabolic efficiency most likely reflecting the reduced energy required to maintain a lower CBT (12).

Reduction of CBT has antiaging effects and prolongs life in poikilotherms (13). In homeotherms, reduction of CBT results from calorie restriction (CR), a controlled dietary regimen that prolongs life span in rodents (14, 15) and that has been reported to delay the onset of a variety of diseases in model organisms (16–21). However, whether re-

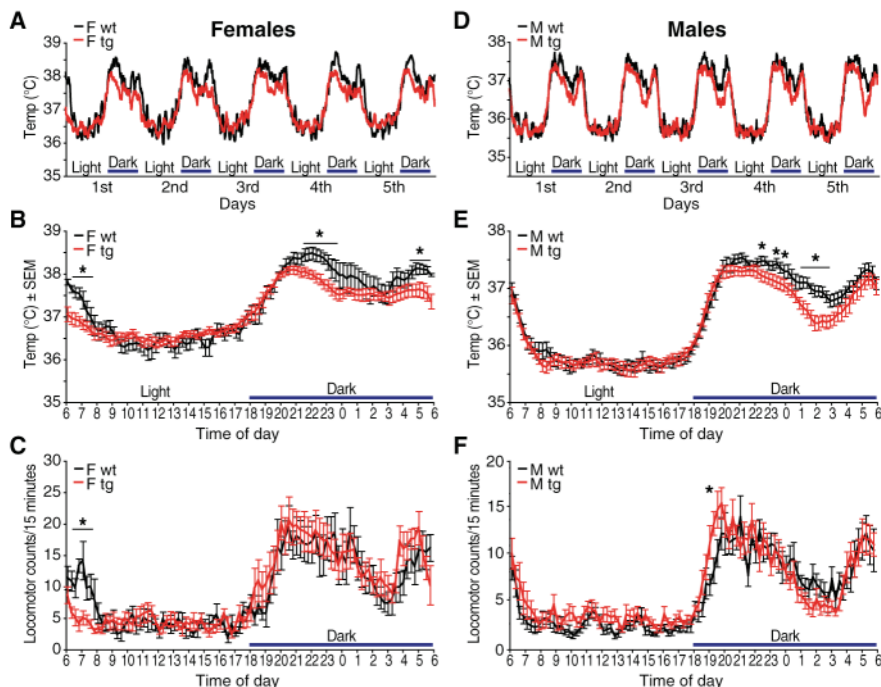
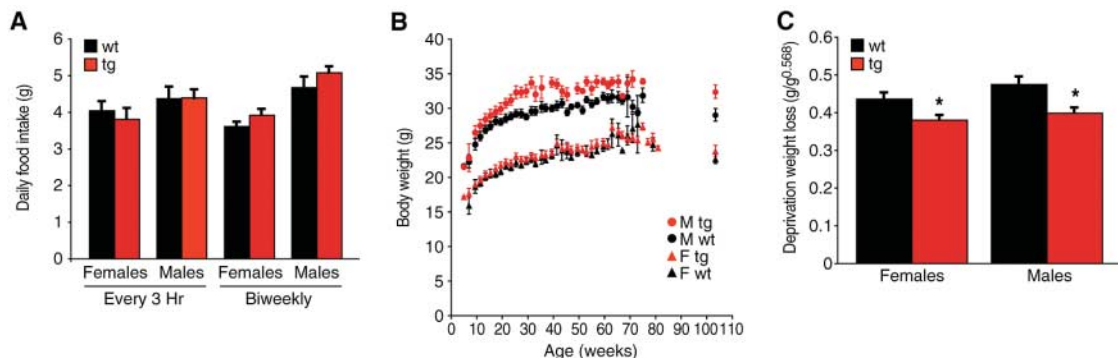


Fig. 2. Core body temperature and motor activity profile. CBT and motor activity were recorded simultaneously on mice implanted intraperitoneally with radiotelemetric transmitters (Data Science International, St. Paul, MN). Mice were allowed to recover for 2 weeks after surgery before recording. The recording was carried out over a period of 10 days. Panels show 5-day temperature profiles (A and D), the average temperature (B and E), and locomotor activity profiles (C and F) from 10 days of 24-hour recording in both male and female mice. The air temperature of the room was maintained at $25 \pm 0.5^\circ\text{C}$ [$n = 15$ mice per group for males, $n = 5$ mice per group for females, $*P < 0.05$ analysis of variance (ANOVA) with repeated measures followed by Fisher's least significant difference (LSD) tests comparing 10-min intervals]. tg, transgenic; wt, wild type.

Fig. 3. Food intake, growth curve, and energy expenditure. (A) Mean ($\pm SEM$) daily chow (11% kcal fat) intake of mice as estimated from measuring food every 3 hours over a 24-hour period or biweekly over a 2-week period (as indicated) in adult age-matched (5 to 6 months old) and weight-matched Hcrt-UCP2 mice ($n = 9$ males and 9 females). Mice from the two genotypes did not differ in their food intake. (B) Growth curve of male and female Hcrt-UCP2 and wild-type littermates determined from biweekly measurements of body weight ($n = 9$ mice per group; $*P < 0.05$ ANOVA). (C) Mean ($\pm SEM$) weight loss after 27 hours of food deprivation in Hcrt-UCP2 and wild-type control mice, normalized for the expected metabolic demands of their predeprivation body



mass as estimated by a power function ($\text{g weight loss/g baseline weight}^{0.568}$) (29). Male and female transgenic mice lost 13 and 16% less weight, respectively, during food deprivation than would have been expected from their metabolic body mass as determined by weight loss of wild-type controls ($n = 6$ and 9, $*P < 0.005$, Fisher's protected LSD test). tg, transgenic; wt, wild-type.

duced CBT in itself prolongs life span in homeotherms has not been demonstrated. To investigate this question, we compared the survivorship of Hcrt-UCP2 mice with wild-type littermates fed ad libitum on an 11% fat (kcal) diet. Despite eating normally (Fig. 3A), the Hcrt-UCP2 genotype showed a 25% reduction in mortality rate across adulthood. As a consequence, life expectancy (median life span from birth) was 89 days (~12%) greater in transgenic as compared with wild-type males and 112 days (~20%) greater in transgenic females (Fig. 4, A and C). Survival was assessed from a total of 57 females and 89 males; six Hcrt-UCP2 males remained alive at the time of this report and were treated as censored observations. Differential mortality was evaluated by Cox proportional-hazard regression with genotype, parent, and sex as main effects and sex-by-genotype as an interaction variable (tables S1 and S2). Each main effect was significant, but there was no effect of sex upon genotype, indicating that UCP2 overexpression in hypocretin neurons has an equal impact on the mortality of both genders.

Inspection of the complementary log-mortality plots between genotypes (Fig. 4, B and D) suggests that the ratio of their hazard rates is approximately constant with time. This assessment was verified by testing the significance of age as a time-dependent covariate; in males and females, there was no evidence to reject the hypothesis that the log mortality plots were parallel (table S3). The mortality rates for the two genotypes were proportional as required for Cox analysis. These data demonstrate that the reduction of CBT within a normal physiological range in Hcrt-UCP2 mice caused a parallel, proportional shift in the mortality rate trajectory, thus reducing the aging-related frailty of the mice (22). This demographic shift resembles the effects of CR upon mortality in mice and poikilotherms and differs from the effects of temperature reduction in poikilotherms, which changes the slope of mortality plots (23–28).

Although the mechanisms underlying the prolonged life span of Hcrt-UCP2 mice have yet to be elucidated, the aggregate data in several ways suggest that the mechanisms may be similar to those mediating the effects of CR. Although the reduction of CBT in Hcrt-UCP2 mice is small, metabolic requirements to maintain a lower CBT are reduced as demonstrated by the increased energy efficiency (Fig. 3C). This may lead to lower oxidative and free radical damage that, over the lifetime, ultimately prolonged life span.

We have shown that a modest and prolonged reduction of body core temperature can contribute to increased median life span in the absence of CR. The Hcrt-UCP2 “cool mice” represent a model for studying mechanisms

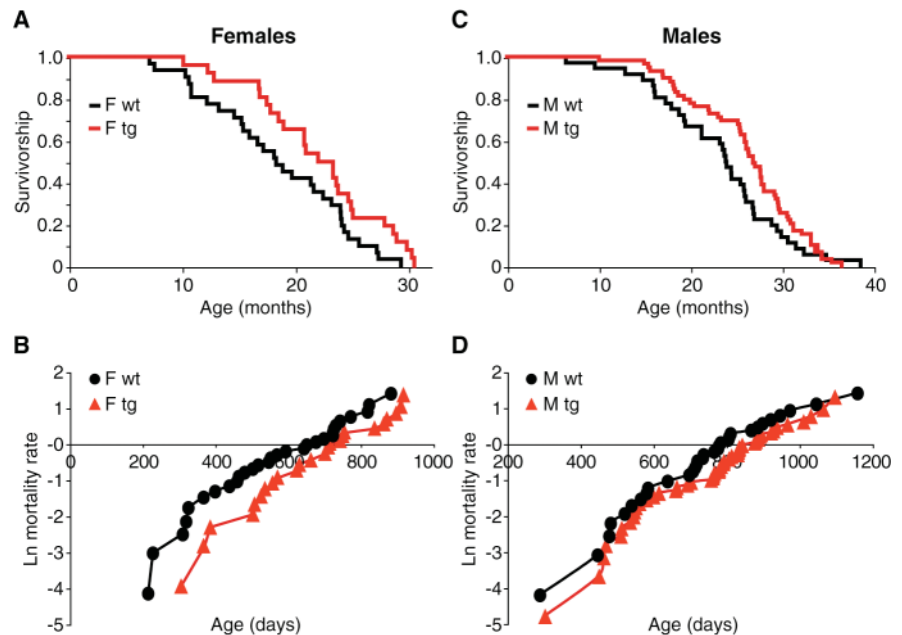


Fig. 4. Survival and mortality curves. Mice were fed ad libitum on sterilized breeder chow. Median life span was (A) 20% (females) and (C) 12% (males) greater in Hcrt-UCP2 mice relative to wild-type littermates. Complementary logarithmic plots (B and D) suggest that the ratio of the hazard rates for Hcrt-UCP2 and wild-type littermates is approximately constant with time. This assessment was verified by testing the significance of age as a time-dependent covariate (table S3). tg, transgenic; wt, wild-type.

underlying thermoregulation and metabolic regulation in mammals. They may also be useful for studying the effects of CBT on aging and longevity that are independent of the effects induced by CR.

References and Notes

1. J. A. Boulant, *Clin. Infect. Dis.* **31** (suppl. 5), S157 (2000).
2. D. Ricquier, F. Bouillaud, *Biochem. J.* **345**, 161 (2000).
3. J. G. Sutcliffe, L. de Lecea, *Nat. Rev. Neurosci.* **3**, 339 (2002).
4. J. T. Willie, R. M. Chemelli, C. M. Sinton, M. Yanagisawa, *Annu. Rev. Neurosci.* **24**, 429 (2001).
5. E. Mignot, S. Taheri, S. Nishino, *Nat. Neurosci.* **5** (suppl.), 1071 (2002).
6. L. de Lecea *et al.*, *Proc. Natl. Acad. Sci. U.S.A.* **95**, 322 (1998).
7. M. Jaszberenyi, E. Bujdosó, E. Kiss, I. Patakai, G. Telegdy, *Regul. Pept.* **104**, 55 (2002).
8. M. Monda, A. Viggiano, F. Fuccio, V. De Luca, *Brain Res.* **1018**, 265 (2004).
9. M. Szekely, E. Petervari, M. Balasko, I. Hernadi, B. Uzsoki, *Regul. Pept.* **104**, 47 (2002).
10. G. Yoshimichi, H. Yoshimatsu, T. Masaki, T. Sakata, *Exp. Biol. Med.* **226**, 468 (2001).
11. J. Hara *et al.*, *Neuron* **30**, 345 (2001).
12. H. C. Chen, Z. Ladhani, S. J. Smith, R. V. Farese Jr., *Am. J. Physiol. Endocrinol. Metab.* **284**, E213 (2003).
13. R. Liu, R. Walford, *Nature* **212**, 1277 (1966).
14. C. McCay, M. Cromwell, L. Maynard, *J. Nutr.* **10**, 63 (1935).
15. R. Weindruch, R. L. Walford, S. Fligiel, D. Guthrie, *J. Nutr.* **116**, 641 (1986).
16. P. H. Duffy, J. E. Leakey, J. L. Pipkin, A. Turturro, R. W. Hart, *Environ. Res.* **73**, 242 (1997).
17. A. Koizumi, M. Tsukada, Y. Wada, H. Masuda, R. Weindruch, *J. Nutr.* **122**, 1446 (1992).
18. W. Duan, M. P. Mattson, *J. Neurosci. Res.* **57**, 195 (1999).
19. D. K. Ingram, R. Weindruch, E. L. Spangler, J. R. Freeman, R. L. Walford, *J. Gerontol.* **42**, 78 (1987).
20. M. P. Mattson, *Brain Res.* **886**, 47 (2000).
21. H. Zhu, Q. Guo, M. P. Mattson, *Brain Res.* **842**, 224 (1999).
22. J. W. Vaupel, K. G. Manton, E. Stallard, *Demography* **16**, 439 (1979).
23. L. Partridge, S. D. Pletcher, W. Mair, *Mech. Ageing Dev.* **126**, 35 (2005).
24. W. Mair, P. Goymier, S. D. Pletcher, L. Partridge, *Science* **301**, 1731 (2003).
25. J. Miquel, P. R. Lundgren, K. G. Bensch, H. Atlan, *Mech. Ageing Dev.* **5**, 347 (1976).
26. M. Parmar, D. Machin, Eds., *Survival Analysis: A Practical Approach* (Wiley, New York, 1995).
27. S. D. Pletcher *et al.*, *Curr. Biol.* **12**, 712 (2002).
28. M. Tatar, *Senescence*, in C. W. Fox, D. A. Roff, D. J. Fairbairn, Eds., *Evolutionary Ecology: Concepts and Case Studies* (Oxford Univ. Press, Oxford, 2001), pp. 128–141.
29. S. N. Austad, D. M. Kristan, *Ageing Cell* **2**, 201 (2003).
30. We thank J. Buxbaum, M. Behrens, M. Brennan, E. Crawford, C. Davis, K. Eusko, R. Fernandez, J. Koziol, M. Martes, T. Hurtado de Mendoza, J. Pemberton, M. Sabbatini, V. Zhukov, and D. Wills for their input and assistance; T. Sakurai for providing the orexin ataxin 3 mice; and M. Tatar for assistance with survival analysis. This work was supported by the Harold Dorris Neurological Research Institute, The Ellison Medical Foundation, NS043501 and MH58543.

Supporting Online Material

www.sciencemag.org/cgi/content/full/314/5800/825/DC1
Materials and Methods
SOM Text
Figs. S1 to S5
Tables S1 to S3
References

7 July 2006; accepted 8 September 2006
10.1126/science.1132191